OXIDATION OF COLUMBIUM AND COATED COLUMBIUM ALLOYS

ARMY MATERIALS AND MECHANICS RESEARCH CENTER

JULY 1973

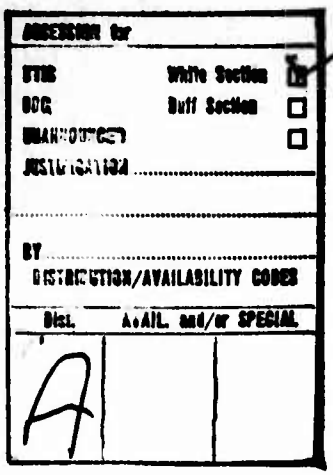

The findings in this report are not to be construed as an official Department of the Army position, unless so designated by other authorized documents.

Mention of any trade names or manufacturers in this report shall not be construed as advertising nor as an official indorsement or approval of such products or companies by the United States Government.

DISPOSITION INSTRUCTIONS

Destroy this report when it is no longer needed.
Do not return it to the originator.

UNCLASSIFIED
Security Classification

DOCUMENT CONTROL DATA - R & D AD-768-153

(Security classification of title, body of abstract and indexing annotation must be entered when the overall report is classified)

1. ORIGINATING ACTIVITY *(Corporate author)*
Army Materials and Mechanics Research Center
Watertown, Massachusetts 02172

2a. REPORT SECURITY CLASSIFICATION
Unclassified

2b. GROUP

3. REPORT TITLE
OXIDATION OF COLUMBIUM AND COATED COLUMBIUM ALLOYS

4. DESCRIPTIVE NOTES *(Type of report and inclusive dates)*

5. AUTHOR(S) *(First name, middle initial, last name)*
Milton Levy, Joseph J. Falco, and Robert B. Herring

6. REPORT DATE	7a. TOTAL NO. OF PAGES	7b. NO. OF REFS
July 1973	~~26~~ 29	19

8a. CONTRACT OR GRANT NO.	9a. ORIGINATOR'S REPORT NUMBER(S)
b. PROJECT NO. D/A 1T162105A328	AMMRC TR 73-35
c. AMCMS Code 612105.11.29400	9b. OTHER REPORT NO(S) *(Any other numbers that may be assigned this report)*
d. Agency Accession No. DA 0B4770	

10. DISTRIBUTION STATEMENT
Approved for public release; distribution unlimited.

11. SUPPLEMENTARY NOTES	12. SPONSORING MILITARY ACTIVITY
	U. S. Army Materiel Command Alexandria, Virginia 22304

13. ABSTRACT

/ Oxidation of columbium alloys FS-85, SU-31, and a complex disilicide coating/ SU-31 and FS-85 alloy systems has been studied in the temperature range 1400 to 2700 F at 1 atm and 50 cm/sec flow rate of air. For studies of the uncoated alloys, the flow rate and pressure dependence of the alloys was also investigated. The experimental methods included thermogravimetric measurements of oxidation rates and studies on reacted specimens by means of X-ray diffraction, metallographic techniques, and electron microprobe analysis. Two anomalies in the temperature dependence of the oxidation rate were observed for both alloys and were related to the oxides formed. The SU-31 alloy has the best oxidation resistance. The oxidation mechanism of the alloys is discussed along with the mechanism of protection afforded by the complex disilicide coating system. The coating did not fail after 1000 hours of oxidation. (Authors)

DD FORM 1 NOV 68 1473 REPLACES DD FORM 1473, 1 JAN 64, WHICH IS OBSOLETE FOR ARMY USE.

UNCLASSIFIED
Security Classification

14 KEY WORDS	LINK A		LINK B		LINK C	
	ROLE	WT	ROLE	WT	ROLE	WT
Columbium alloys Oxidation Protective coatings Gas turbine engines Helicopters						

☆U.S. GOVERNMENT PRINTING OFFICE: 1973–70056/43

AMMRC TR 73-35

OXIDATION OF COLUMBIUM AND COATED COLUMBIUM ALLOYS

Technical Report by

MILTON LEVY, JOSEPH J. FALCO, and ROBERT B. HERRING

July 1973

D/A Project 1T162105A328
AMCMS Code 612105.11.29400
Metals Research for Army Materiel
Agency Accession Number DA 0B4770

Presented at Tri-Service Corrosion Conference, Houston, Texas, 5-10 December 1972.

METALS RESEARCH DIVISION
ARMY MATERIALS AND MECHANICS RESEARCH CENTER
Watertown, Massachusetts 02172

AMMRC Ex. O. 33A12

ARMY MATERIALS AND MECHANICS RESEARCH CENTER

OXIDATION OF COLUMBIUM AND COATED COLUMBIUM ALLOYS

ABSTRACT

Oxidation of columbium alloys FS-85, SU-31, and a complex disilicide coating/SU-31 and FS-85 alloy systems has been studied in the temperature range 1400 to 2700 F at 1 atm and 50 cm/sec flow rate of air. For studies of the uncoated alloys, the flow rate and pressure dependence of the alloys was also investigated. The experimental methods included thermogravimetric measurements of oxidation rates and studies on reacted specimens by means of X-ray diffraction, metallographic techniques, and electron microprobe analysis. Two anomalies in the temperature dependence of the oxidation rate were observed for both alloys and were related to the oxides formed. The SU-31 alloy has the best oxidation resistance. The oxidation mechanism of the alloys is discussed along with the mechanism of protection afforded by the complex disilicide coating system. The coating did not fail after 1000 hours of oxidation.

CONTENTS

INTRODUCTION

Stoichiometric burning of the fuel in a turbine engine can produce turbine inlet temperatures (TIT) in excess of 3000 F, but the current nickel-base and cobalt-base superalloys used for blades and vanes in the turbine section are limited by creep strength and oxidation resistance to operation at 1800 to 1900 F metal temperature. Since gas temperatures of 2200 to 2250 F at the turbine inlet are used in current Army turbine engine designs, sufficient cooling air must be diverted from the compressor section through complex passages to cool the blades and vanes to their permissible operating temperature range.

A substantial increase in turbine horsepower and improvement of fuel economy could be achieved by increasing the TIT to the 2500 to 2600 F range. With currently used nickel-base alloy materials such an increase in TIT would necessitate the adoption of transpiration-cooled blade and vane designs and would require substantially more cooling air than is now used for that purpose. The diversion of more air from the compressor and its introduction into the turbine for cooling would tend to cancel out the benefits of the higher turbine inlet temperatures.

The use of coated refractory metal alloys offers an alternative to the transpiration-cooled blade design. Refractory metal alloy components with substantially higher melting temperatures than nickel-base alloys could maintain adequate creep strength at temperatures up to 2600 F. Of the refractory metal alloys, columbium alloys appear the most promising candidates because of their favorable strength-to-weight ratios. However, like other refractory metal alloys, columbium alloys lack the intrinsic oxidation resistance to operate for long periods of service without a protective coating. While work is in progress to develop improved coatings for columbium alloys, it must be expected that there will be a certain incidence of coating failures (due to foreign object damage or other causes). In the case of a coating failure, the underlying substrate may be subjected to oxidation. Thus, the most oxidation-resistant alloy should be utilized.

This study was undertaken to assess in s. detail the oxidation behavior of a new commercial columbium-base alloy, SU-31, which has shown good mechanical properties. For comparison, some data is also reported on an older commercial columbium-base alloy, FS-85. In addition, the oxidation behaviors of complex disilicide coating/SU-31 and FS-85 systems were studied.

PAST WORK

The oxidation of pure columbium has been extensively studied and found to be complex.[1,2] The more interesting features of the kinetics involve two rate anomalies[2] which occur for pure columbium in the range near 1100 F (593 C) and 1600 F (871 C).

At temperatures below 1200 F (649 C) the oxidation proceeds in a parabolic form during a pretransition period followed by a transition or breakaway into a linear kinetic range at longer times. Hurlen[3] found that the kinetics below 1200 F during the pretransition region could be further divided into an initial linear stage (I) followed by a parabolic stage (II). Other investigators have reported only the approximately parabolic kinetics[1] (Hurlen's region II).

A generalized oxidation weight gain curve for pure columbium exposed below 1200 F is shown in Figure 1 drawn according to the observations of Hurlen.[3] There are several oxidation stages which are described as I - linear, II - parabolic, III - linear, IV - parabolic, and V - parabolic with transitions between them. The transition between parabolic II and linear III is most pronounced and most interesting since it represents a transition from a protective to a nonprotective type of oxidation. Under the relatively short experimental time periods used in this study, it was not possible to observe all of these types of oxidation in any single run.

Hurlen[3] identified the initial linear stage I with oxygen being dissolved in the metal and found the initial linear oxidation proportional to the square root of the oxygen pressure at low pressures (below 1 torr) and independent of pressure at higher oxygen pressures. From this dependence Kofstad[1] concluded that the stage I (initial) mechanism involves a dissociative absorption of oxygen followed by incorporation of oxygen in columbium. The parabolic stage II in the pretransition region is essentially pressure independent[3] and Kofstad[1] attributed most of the weight gain in this range to oxygen dissolution, assuming an oxygen concentration of 5 atomic percent at the metal surface. The observed activation energies[4] for the parabolic range have been reported as 27.4 Kcal/mol and 22.8 Kcal/mol which are in good agreement with values reported for oxygen diffusion in columbium.[5,6]

The parabolic range II also has been identified with the formation of CbO_x and CbO_z suboxide phases. CbO_x is a tetragonal phase, closely related to the metal structure, and is only formed below 840 F (450 C).[1] Brauer et al.[7] have

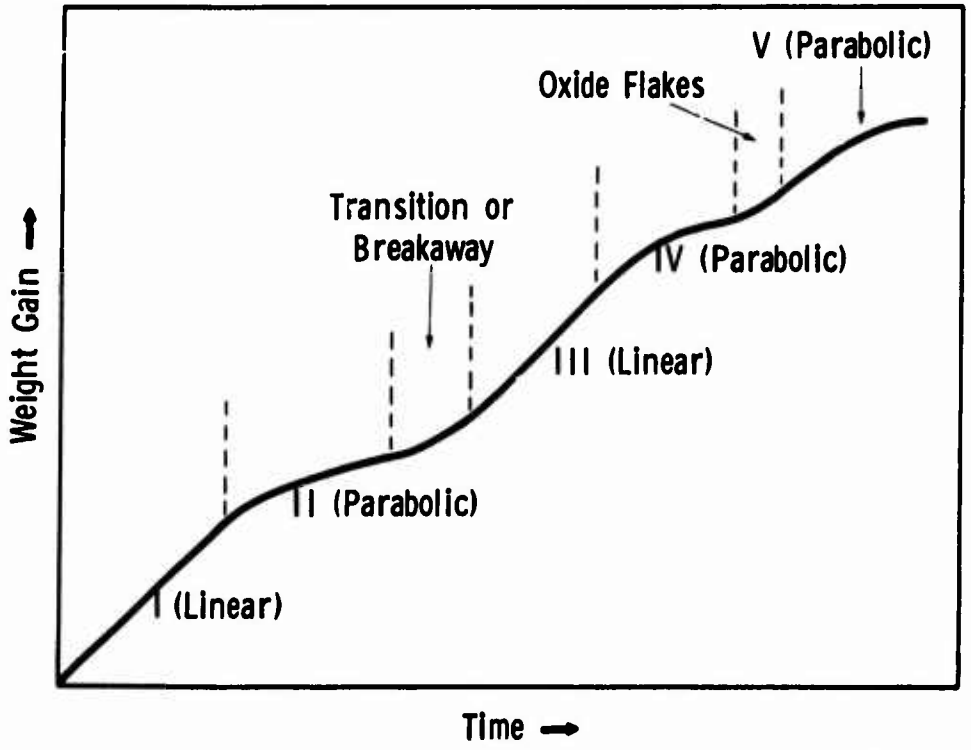

Figure 1. Generalized oxidation - time curve for columbium (after Hurlen[3]).

suggested possible formulas of Cb_6O and Cb_5O. Suboxide CbO_z, also tetragonal with a unit cell approximately six times that of the metal, decomposes above 1100 F (593 C)[7] and is not an intermediate oxidation product above that temperature.

During the transition to the accelerated kinetics of stage III in Figure 1, the first nuclei of Cb_2O_5 are reported to form[1] and breakaway is reported to be associated in some way with formation of Cb_2O_5 which is porous and offers little or no resistance to further oxidation. The duration of the pretransition region (stages I and II) becomes progressively shorter with increasing temperature. Above 500 C (932 F) it is too short to be evaluated in standard thermogravimetric studies.[1] Pawel et al.[8] have shown that the time to onset of the breakaway transition to linear oxidation is strongly influenced by the crystallographic orientation of the metal. The stage following the breakaway is commonly described as linear but deviations from linear have been reported. Cox and Johnston[9] found that the rate was more rapid than linear just following the transition but that it soon decreased toward linear kinetics. A more rapid than linear kinetics of oxidation at the start of breakaway may reflect rapid nucleation and growth of Cb_2O_5.[1] Later, when a thick oxide film has formed, the oxide may behave as a barrier to flow of oxygen to the metal surface, causing a reduction in kinetics to somewhat below linear.[1] The two final approximately parabolic stages IV and V, shown in Figure 1, probably reflect this behavior rather than solid-state diffusion limited processes.

Above 1200 F (649 C) the initial oxidation is parabolic followed by a transition to approximately linear oxidation kinetics. At these temperatures CbO_2 is not stable and the oxidation to Cb_2O_5 proceeds by the formation of the suboxides CbO and CbO_2, and according to Kofstad[1] involves the steps Cb → Cb - O (sol. soln) → CbO → CbO_2 → Cb_2O_5.

It has been found by precision lattice parameter measurements[10] that above 1200 F there is less oxygen concentration in the metal beneath the oxide/metal interface than at lower temperatures. Kofstad[1] has suggested that above the temperature where CbO and CbO_2 appear, the oxygen level at the metal/oxide interface is decreased to a low value in equilibrium with CbO.

The CbO phase is grey with a metallic luster and has been reported to have a defective sodium choloride structure with the (0,0,0) and (1/2,1/2,1/2) sites vacant.[1] CbO_2 is black and has a structure related to the rutile structure. Low pressure oxidation studies reported by Inouye[11] and by Kofstad and Espevik[12] showed that CbO does not form a plane film or scale on the metal, but grows as irregularly shaped crystals and as such does not have protective properties. CbO_2, however, forms a compact protective scale.[12]

The linear stage of oxidation above 1200 F appears to be well identified with the formation of a porous layer of Cb_2O_5.[1] The Cb_2O_5 is white when stoichiometric but darkens appreciably on departures from stoichiometry.[3] Several polymorphic modifications have been reported, but generally those can be considered in terms of a low temperature (T or γ) form, an intermediate temperature (M or β) form, and a high temperature (H or α) form with the transition from the intermediate to the high temperature form occurring about 830 C (1526 F). The latter transformation is irreversible and somewhat dependent on heating rate.[13] From these

observations Goldschmidt has concluded that the intermediate temperature form of Cb_2O_5 is probably a metastable phase. While the crystal structures of all of the Cb_2O_5 allotropes have not been determined, those which have been determined have been indexed on the basis of a monoclinic unit cell.

In an earlier study Levy and Falco[14] reported that a modified complex disilicide coating afforded a 90Ta-10W alloy complete protection against static oxidation for at least 200 hours at temperatures between 1700 and 2700 F. That data warranted the selection of the silicide coating for this study.

EXPERIMENTAL PROCEDURE

Materials

The columbium alloy SU-31 was developed by Imperial Metal Industries of Great Britain. The material for this study was obtained through Kawecki-Berylco Industries, Inc.,* which holds the license for production and distribution of SU-31 in the United States. The alloy, obtained in the form of 1/2-inch-diameter rod, had been given a final precipitation strengthening heat treatment of 1 hour at 1600 C followed by 1 hour at 1200 C.

Oxidation specimens in the form of short cylinders were cut from the rod and surface ground to a thickness of 0.125 $\pm$ .001 inch (0.318 cm).

The FS-85 columbium-base alloy was obtained from Fansteel Corp.† in the form of 0.125-inch-thick (0.318 cm) sheet. The sheet was cut into 1/2-inch squares.

Prior to an oxidation test, the specimen was polished on metallographic paper through 2/0 grade, cleaned in acetone, and rinsed in distilled water.

Table 1 shows the nominal composition and chemical analysis of the alloys. Figure 2 shows the microstructures of the FS-85 and SU-31 alloys. Note the banding and the intergranular precipitate for the FS-85 alloy which is probably ZrO_2. Note the stringers of columbium-rich carbide particles in the SU-31 alloy. This alloy is a carbide dispersion strengthened alloy (high carbon content, listed in Table I). For the coating study, oxidation specimens of both alloys were coated with a modified silicide by Solar‡ employing the procedure described in Table II.

Oxidation of Uncoated Alloys - Weight Gain

Weight gain measurements during isothermal oxidation tests were made using a Mettler Thermogravimetric Balance. Specimens were brought to temperature in an argon atmosphere and time was measured from the introduction of flowing air in the specimen chamber. The apparatus and procedure has been previously described in detail.[14] One-hour oxidation tests were conducted for uncoated SU-31 and FS-85 specimens at temperatures between 1000 F and 2700 F at several air flow

*Kawecki-Berylco Industries, Inc., 220 E. 42nd St., New York, N.Y. 10017
†Fansteel Corp., 5101 Tantalum Place, Baltimore, Maryland 21226
‡Solar, Division of International Harvester Co., San Diego, California

Table I. COMPOSITION OF THE ALLOYS

	Element	Nominal (wt. %)	Analysis (wt. %)
SU-31	Tungsten	17.0-18.0	18.50
	Hafnium	3.5	3.60
	Carbon	0.12	0.145
	Oxygen	--	85ppm
	Nitrogen	--	25ppm
	Columbium	Bal.	Bal.
FS-85	Tantalum	27.0	27.60
	Tungsten	11.0	10.60
	Zirconium	1.0	0.94
	Hafnium	--	100ppm
	Molybdenum	--	100ppm
	Titanium	--	50ppm
	Iron	--	50ppm
	Silicon	--	50ppm
	Carbon	--	40ppm
	Oxygen	--	39ppm
	Nitrogen	--	29ppm
	Hydrogen	--	5ppm
	Columbium	Bal.	Bal.

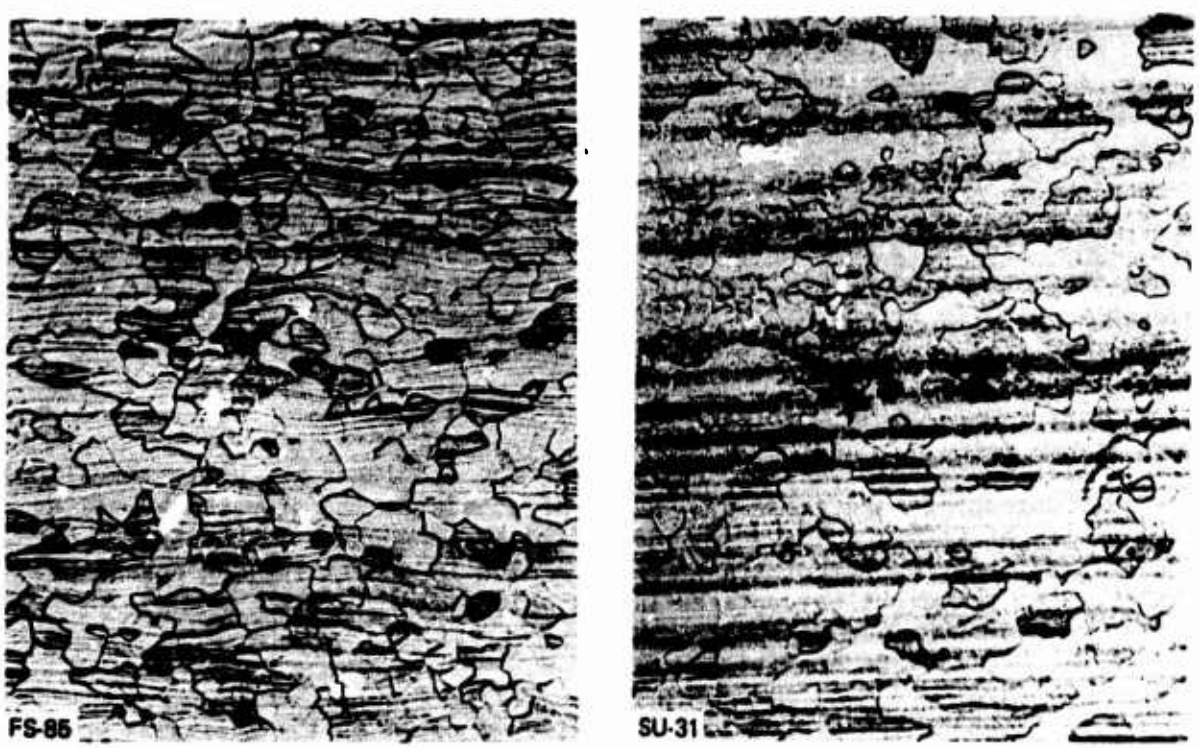

19-066-1599/AMC-72

Figure 2. Microstructures of as-received alloys (etched). Orig. Mag. 250X

Table II. APPLICATION PROCEDURE FOR SOLAR DUPLEX COATING NS-4/Si

1. Barrel Finish
2. Vapor degrease
3. Sandblast
4. Pickle (acid etch-rinse)
5. Spray with NS-4 coating (50W, 20Mo, 15V, 15Ti)
6. Dry
7. Sinter at 2780 F ± 30 F at 10^{-15} torr for 15 hours
   - Weight gain 55 to 65 mg/cm^2 (NS-4)
   - Thickness increase 4.5 to 5.0 mils/surface (NS-4)
8. Silicide at 2150 F to 800 torr argon for 16 hours or equivalent
   - Weight gain 34 to 40 mg/cm^2 (silicide)
   - Thickness increase 2.8 to 3.3 mils/surface
9. No post clean
10. Post-oxidation at 2400 F for 1 hour

Note: Total thickness increase was 7.0 to 8.5 mils/surface

rates. Limited tests were carried out at reduced pressure. For the coated alloys, oxidation runs were of 200 hours duration. The reacted specimens were examined by means of metallographic, X-ray fluorescence, X-ray diffraction, and electron microprobe analyses.

Metallography

The specimens from the weight gain tests described above were mounted in bakelite and ground to expose a cross section through the center of the sample. The specimens were polished on metallographic papers through the 600 grit and finished on a vibratory polisher using Linde A slurry for 6 hours and Linde B for an additional 6 hours.

A few SU-31 disk specimens, which were oxidized for periods up to 32 hours, were sectioned using a spark cutting machine and the two halves were glued face-to-face. They were mounted to expose the cut surfaces and polished as above. The edge definition at the metal-oxide interface was improved by this technique. The etch used to reveal the structure was composed of the following: 50 ml HF, 50 ml H_2SO_4, 5 ml H_2O_2, and 85 ml H_2O.

X-ray Fluorescence Analysis

Analysis of the oxides from several of the specimens was performed using X-ray fluorescence spectroscopy. A set of standards was prepared by mixing varying ratios of Cb_2O_5, Ta_2O_5, HfO_2, ZrO_2, and WO_3 powders. Intensity ratios determined from the set of standards were used in converting the observed intensities to weight percentages in the oxides.

X-ray Diffraction Analysis

X-ray diffraction analyses of the oxides present on the specimens were obtained using a Norelco diffractometer. A copper target X-ray tube was used and the diffractometer was operated at a scan speed of one degree per minute.

Lattice plane "d" spacings observed were compared with values reported in the ASTM powder index card file.

At temperatures of 1600 F and below, the oxides were relatively adherent and diffraction patterns were usually obtained from the oxides still attached to the specimen. At temperatures of 1800 F and above, all the loose oxide and that which could be removed by scraping was collected, powdered, and mounted for diffraction.

Electron Microprobe Analysis

Electron microprobe analysis of coated alloys was performed with an AMR electron beam microanalyzer. The V, Ti, Mo, Hf, W, Cb, and Si concentrations were determined for the microconstituent phases present in the coating and in the substrate alloy. The concentration distributions of these elements were recorded as a function of distance across the coating.

RESULTS

Weight Gain Measurements

Double logarithmic plots of weight gain vs. time for the oxidation of SU-31 at atmospheric pressure and at various temperatures are shown in Figure 3. At 1000 and 1200 F the oxidation follows a linear rate. Comparison of the 1200 and 1400 F curves shows that there is an increase in weight gain with temperature at any given time but the slope of the 1400 F curves is less, namely, 0.43, indicating approximate parabolic kinetics. Oxidation continues to follow an approximate parabolic rate up to temperatures of 2200 F for times under one hour. The shift from linear kinetics at 1200 F to parabolic kinetics at 1400 F with concomitant reduction in rate is the low temperature anomaly in the temperature dependence of the oxidation rate.

A second or high temperature anomaly occurred in the range 1800 to 2000 F where the 2000 F curve falls below that for 1800 F. At temperatures above and below this range, an increase in temperature resulted in an increase in oxidation weight gain for equal times.

At 2200 F oxidation follows the parabolic rate law throughout the entire run. At 2400 and 2600 F oxidation is parabolic for the first 20 minutes after which it becomes linear. Results similar to those shown in Figure 3 for flow rates of 100 cm/sec were also observed in tests conducted at flow rates of 50 cm/sec.

Similar double logarithmic plots for the FS-85 alloy are shown in Figure 4. The kinetics of oxidation at 1000 F were near parabolic in the time to one hour, while the curves for 1200, 1300, and 1400 F begin with a slope of near 0.5 but increase in slope at times beyond 20 minutes to values greater than one. There was no change in slope at 1600 F where oxidation was essentially linear. Above 1600 F the first or lower temperature rate anomaly occurred, resulting in a decrease in slope of the curves for the higher temperature tests.

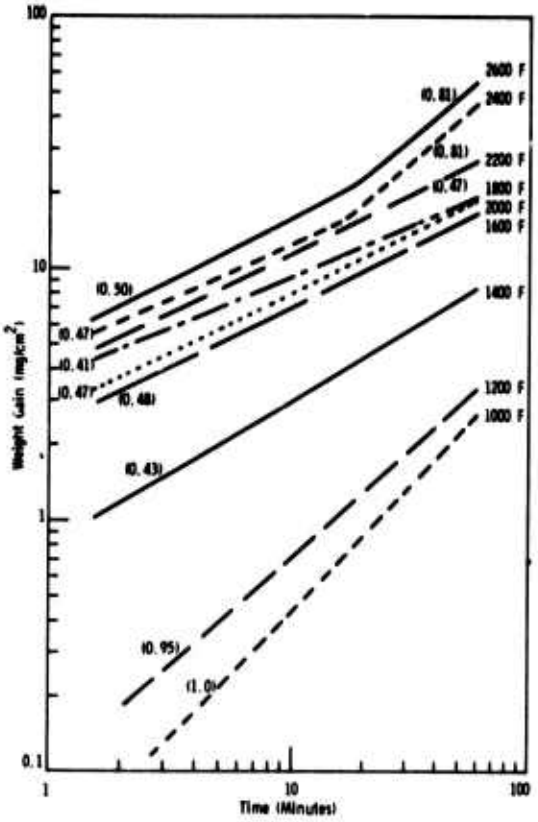

Figure 3. Oxidation of SU-31 between 1000 and 2600 F at an air flow rate of 100 cm/sec

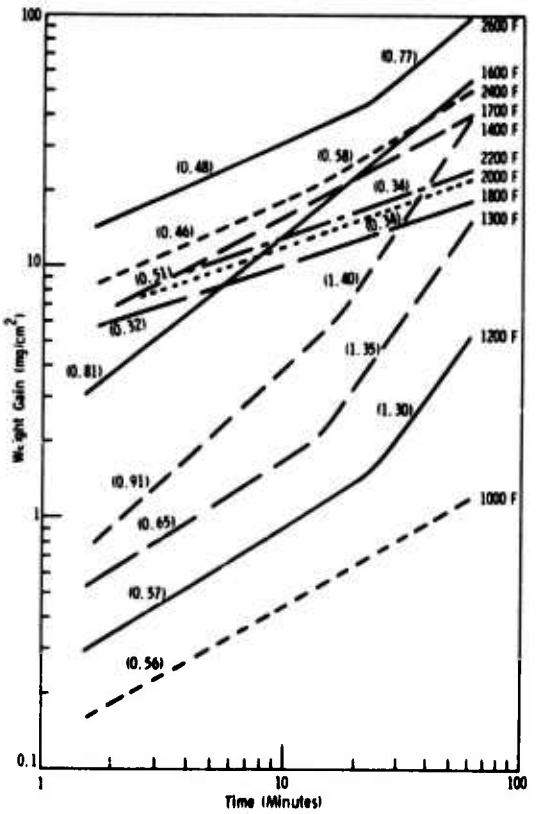

Figure 4. Oxidation of FS-85 between 1000 and 2600 F at an air flow rate of 100 cm/sec

The second or higher temperature rate anomaly occurred in the range 1700 to 1800 F and resulted in weight gains decreasing with increasing temperature for equal times. From 1800 to 2600 F weight gains again increased with temperature. The curve for 2600 F shows the transition from parabolic to near-linear kinetics after about 20 minutes which was observed in the 2400 and 2600 F runs for the SU-31 alloy. Results very similar to those shown in Figure 4 were also obtained in tests at a reduced flow rate of 50 cm/sec.

Figure 5 compares the oxidation of SU-31 with FS-85 as a function of temperature. Generally, SU-31 is more oxidation resistant than the FS-85 alloy. Major differences in oxidation rate occur between 1400 and 1600 F and above 2200 F. Between 1400 and 1600 F FS-85 exhibits markedly greater oxidation rates, i.e., linear oxidation as opposed to parabolic for the SU-31 alloy. Above 2200 F the FS-85 alloy changes from parabolic to linear kinetics sooner than the SU-31 which may account for its greater oxidation rates. The oxidation rates appear to be comparable in the range between 1800 and 2200 F where the kinetics for both alloys is parabolic. Note that both alloys have weight gains in excess of 20 mg/cm^2 at temperatures above 2000 F for 1 hour. An acceptable value would be ∿15 mg/cm^2 for 200 hours or ∿25 mg/cm^2 for 1000 hours. Thus neither alloy would have adequate oxidation resistance at these temperatures.

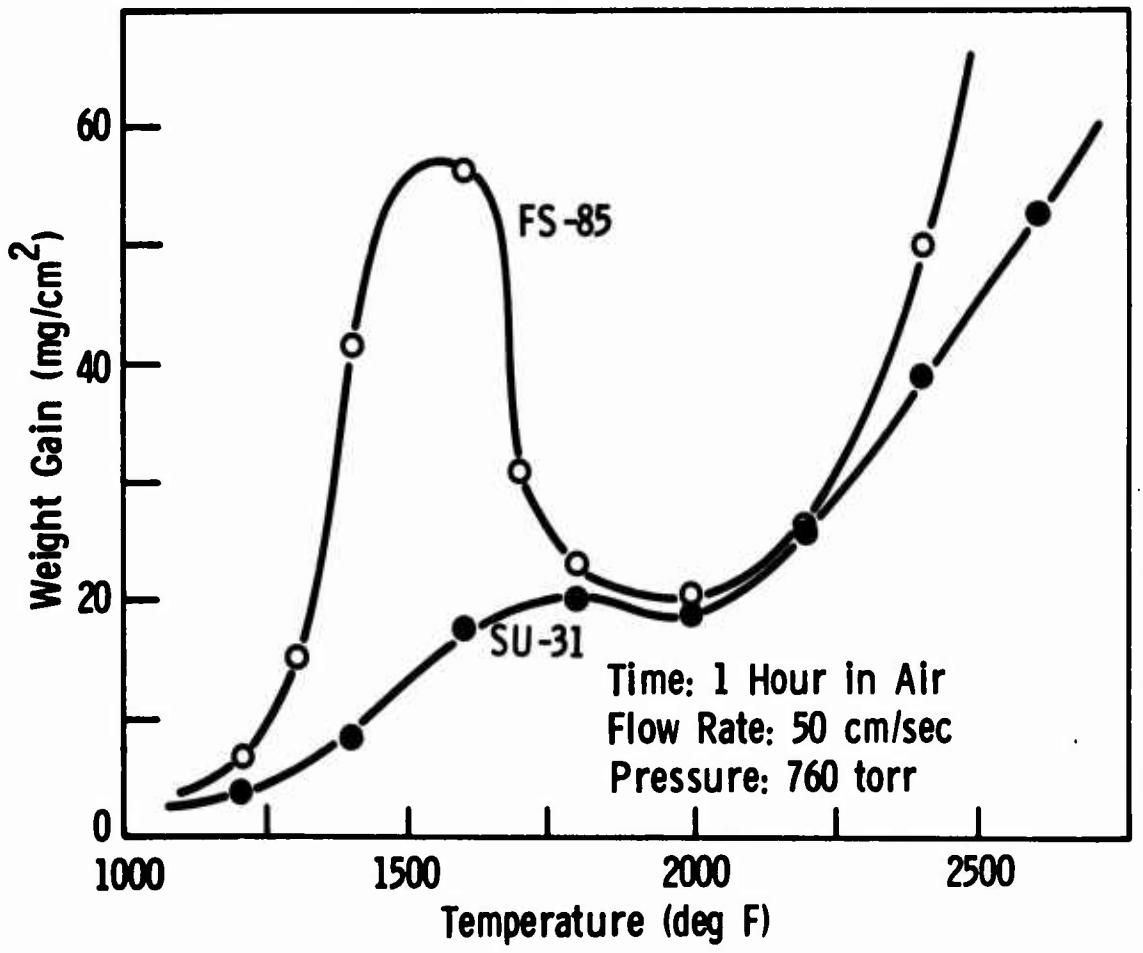

Figure 5. Comparison of SU-31 and FS-85 oxidation after one hour at temperatures between 1200 and 2700 F

Figure 6 shows the effect of pressure and air flow rate on the oxidation behavior of SU-31 at several temperatures. Oxidation rates increase with increasing temperatures. At all temperatures, increases in air flow rate and pressure produce increases in oxidation rate. Thus the reaction is limited by the supply of oxygen reaching the alloy. The effect of pressure and air flow becomes more pronounced the higher the temperature.

Appearance of the Oxides

The oxides formed on the FS-85 specimens after one hour at temperatures of 1000 to 1600 F consisted of a dark inner layer adhering to the metal and an outer white powdery layer. A section through the inner scale on the FS-85 alloy oxidized one hour at 1600 F is shown in Figure 7. Only the inner layer is shown, the loose outer powder having been lost during the mounting of the specimen. However, at 1800 F and above, the outer layer sintered into a porous compact which was retained on the specimens mounted for metallography. A cross section of the scale on a specimen of FS-85 oxidized for one hour at 2600 F is shown in Figure 8. A crack between the porous outer layer and the dense inner layer and cracks in the porous outer layer are observed. These cracks probably developed during cooling due to thermal stress. The small dark spots in the inner oxide layers shown in Figures 7 and 8 are voids.

The oxide scale on the SU-31 alloy following oxidation at 1600 F and above was of a two-layer type. The thin inner layer was compact and dark bluish-black while the outer layer was light yellow in color immediately after oxidation but turned light green upon standing in air for a few days at room temperature. The oxide scale on SU-31 was thinner than that on the FS-85 for comparable temperatures and times. Upon cooling from 1800 F and above, the outer portion of the

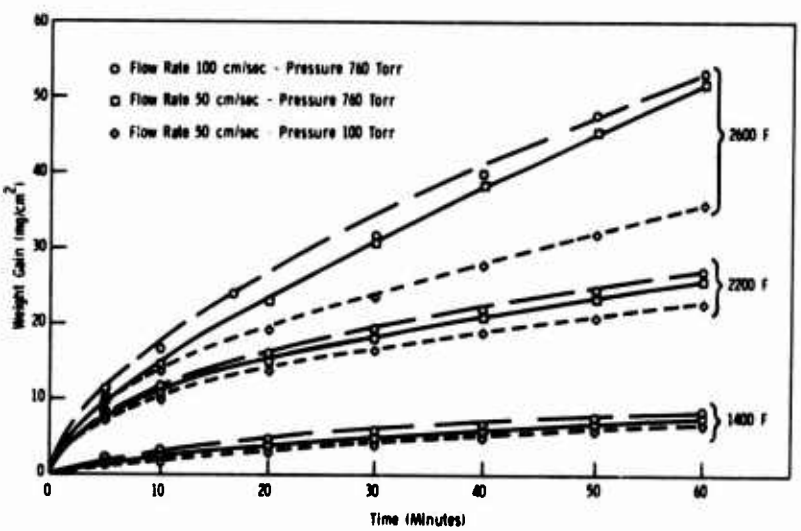

Figure 6. Effect of pressure and flow rate on oxidation of SU-31

Figure 7. Cross section of oxides formed on FS-85 after 1 hr at 1600 F

19-066-1589/AMC-72

Figure 8. Cross section of oxides formed on FS-85 after 1 hr at 2600 F

19-066-1592/AMC-72

SU-31 oxide spalled from the specimens, leaving only a very thin (∿20μ) dark inner layer attached to the underlying metal. The oxide on a specimen oxidized for one hour at 1600 F is shown in Figure 9. Porosity in the outer layer can be noted along with the thin dark layer at the oxide/metal interface.

X-Ray Fluorescence Analysis

Samples of the oxide scales from the FS-85 and SU-31 specimens were removed from the metal, powdered, and subjected to X-ray fluorescence analysis. The resulting elemental fluorescent intensities were interpreted assuming the constituent elemental oxides comprised 99% or more of the powder. Both intensity ratios and oxide weight ratios were referred to columbium oxide using a set of calibration curves generated for mixtures of simple oxides. This technique helps to eliminate the effects of variation of sample size, particle size, density, and area exposed to the primary X-ray beam and compensates for interelemental effects.[15]

Table III shows the analysis of the oxide on SU-31 alloy exposed at 1600, 1800, 2200, and 2600 F. Table IV shows results for the FS-85 alloy exposed at 1600, 2000, and 2400 F.

Generally, Cb_2O_5 was the major constituent of the scales of both alloys at temperatures between 1600 and 2600 F. However, the technique does not permit differentiation between the various forms of Cb_2O_5 present. For the SU-31 alloy, the oxide scale contained a relatively small amount of HfO_2. ZrO_2 was identified as a minor constituent of the scale of the FS-85 alloy. In both cases, amounts were too small (<3.5%) to be detected by X-ray diffraction analysis. It is possible that some of the compounds identified were also present in a combined form such as 6 $Cb_2O_5 \cdot WO_3$ ($Cb_{12}WO_{33}$).

Orig. Mag. 500X

Figure 9. Cross section of oxides formed on SU-31 after 1 hr at 1600 F

19-066-1593/AMC-72

Table III. X-RAY FLUORESCENCE ANALYSIS OF SURFACE OXIDE ON SU-31 ALLOY (in weight percent)

Temperature (F)	Cb_2O_5	WO_3	HfO_2
1600	87.7	9.7	2.6
1800	76.6	20.0	3.4
2200	77.8	18.9	3.3
2600	78.3	18.5	3.2

Table IV. X-RAY FLUORESCENCE ANALYSIS OF SURFACE OXIDES ON FS-85 ALLOY (in weight percent)

Temperature (F)	Cb_2O_5	Ta_2O_5	WO_3	ZrO_2
1600	68.0	26.1	5.7	0.2
2000	53.0	39.0	8.0	1.0
2400	55.0	36.0	8.0	1.0

Phase Identification by X-Ray Diffraction

Rather extensive work on the identification of compounds in the Cb_2O_5-WO_3 oxide system has been reported by Roth and Wadsley.[16] Their work permitted the identification of complex oxides to be made from X-ray diffraction patterns for the SU-31 reaction products.

At temperatures below 1800 F, the oxide found on the surface following a one-hour exposure in air was adherent. X-ray diffraction patterns of the oxide layer while still attached to the substrate showed the presence of two predominant compounds: the intermediate temperature form of Cb_2O_5 (M or β) (5-0352) and $Cb_{12}WO_{33}$ (or $6Cb_2O_5.WO_3$) (18-930). The numbers in parentheses refer to the ASTM Powder Pattern file numbers of the identified compounds. Small amounts of CbO_2 (17-717) were also identified in the specimens exposed at 1400 F and above. CbO_2 was not present in the patterns for specimens exposed at 1000 and 1200 F. The observed lattice plane spacings for the patterns obtained from the specimens exposed at 1600 and 1800 F are presented in graphical form in Figure 10a as a spectral representation in which the position of the lines indicates "d" spacing of observed diffraction peaks and the relative height is related to the relative peak intensity. ASTM standard patterns for the identified phases are also shown and peak identifications are indicated by dotted line connections.

The thicker oxide developed on an SU-31 specimen exposed for 16 hours at 1600 F was less adherent than that on the one-hour specimen and was readily removed from the metal. An attempt was made to separate the light yellow oxide (equivalent to that found in the outer layer of the freshly reacted specimen) from the dark-colored oxide (equivalent to the thin layer adjacent to the substrate). X-ray diffraction patterns of those two samples again indicated the presence of the intermediate temperature βCb_2O_5 (5-0352), $Cb_{12}WO_{33}$ (18-930), and CbO_2 (17-717) phases. By comparison of intensities of peaks in the samples from the inner dark layer and the outer light layer it was confirmed that the dark phase near the metal surface was the CbO_2. However, in addition, four weak peaks

appeared in the outer oxide pattern which have been identified as belonging to the higher temperature form of αCb_2O_5 (16-053).

In the temperature range 2000 to 2200 F, the oxide was less adherent and spalled from the surface on cooling. The oxide was removed from the sample and powdered prior to X-ray diffraction studies. At both 2000 and 2200 F, peaks were identified as belonging to the higher temperature polymorphic form of αCb_2O_5 (16-053) and the $Cb_{12}WO_{33}$ ($6Cb_2O_5.WO_3$) (18-930) phases. Relative peak intensities indicated that $Cb_{12}WO_{33}$ was the predominant phase. The observed lattice plane spacings for the samples oxidized at 2000 and 2200 F are shown in Figure 10b as a spectral representation and the observed patterns are compared with the reported patterns for the phases identified.

The oxides formed in one hour at 2400 and 2600 F also spalled on cooling. They were removed from the substrate and powdered prior to examination by X-ray diffraction. The patterns obtained were quite different from those at the lower temperatures and the phases present have been identified as $Cb_{14}W_3O_{44}$ ($7Cb_2O_5.3WO_3$) (18-929) and $Cb_{26}W_4O_{77}$ ($13Cb_2O_5.4WO_3$) (20-1319). The data are shown graphically in spectral form in Figure 10c.

For the oxide found on the FS-85 alloy in the range 1000 to 1600 F the diffraction pattern was similar to that of the intermediate temperature βCb_2O_5 (5-0352). However, the peaks were slightly shifted indicating that one of the alloying elements, probably tantalum, is incorporated in the oxide. In addition, some weaker peaks remain unidentified which may belong to a Cb-Ta-W oxide phase. The phase CbO_2 was absent from patterns for specimens exposed at 1000, 1200, and 1400 F. The principal peak for CbO_2 (17-717) was detected weakly in the pattern for the 1600 F specimen and was stronger in the patterns for 1700 F and above.

In the range 1700 to 2600 F the predominant phase was similar to the diffraction pattern for the higher temperature form of αCb_2O_5 (16-053). Peaks identified as CbO_2 were also present along with some unidentified peaks which may belong to Cb-Ta-W oxide phases.

Figure 11 shows the effect of temperature on the surface hardness increase for SU-31. The values for surface hardness increase, decrease with temperature, particularly in the temperature range between 1800 and 2200 F which implies a decrease in the level of oxide contamination at the oxide/metal interface. This effect is not clearly related either to the transition from the βCb_2O_5 to αCb_2O_5 or to the presence of the complex oxides such as $Cb_{12}WO_3$. Nevertheless, the oxidation rates were parabolic in the temperature range of 1800 to 2200 F where there was a decrease in the level of oxide contamination.

Oxidation of the Coated Alloys

Weight Gain Study

It should be noted that a post-oxidation treatment described in Table II was given to those coated specimens which were being oxidized in the pesting range (1400 to 1600 F). Falco and Levy[17] developed a post-oxidation treatment which

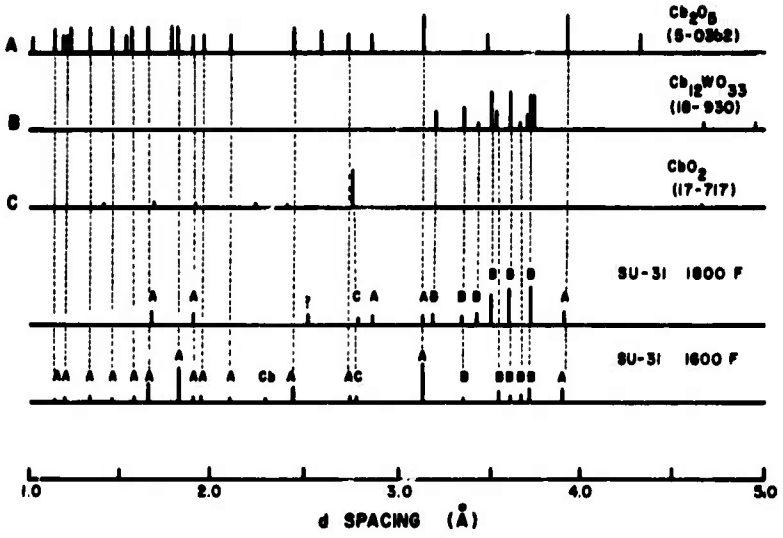

a. Oxidation at 1600 and 1800 F

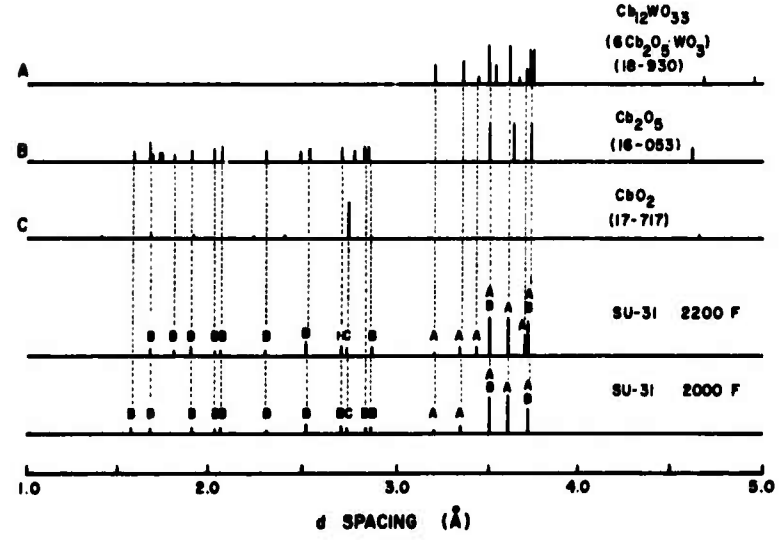

b. Oxidation at 2000 and 2200 F

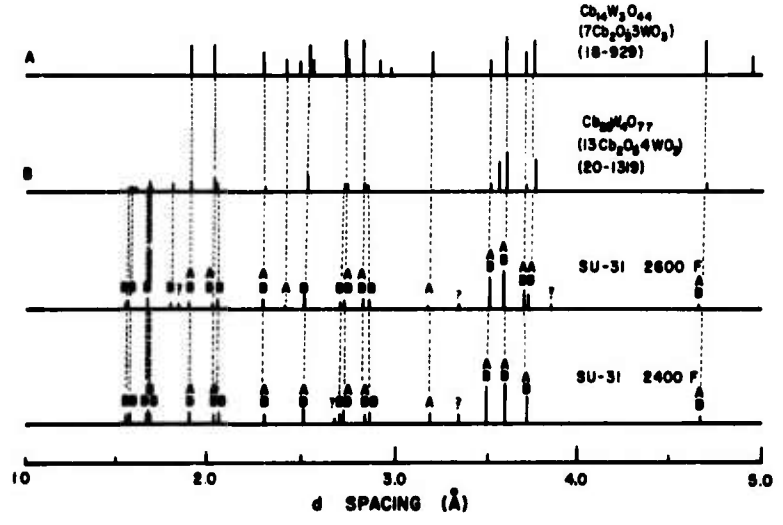

c. Oxidation at 2400 and 2600 F

Figure 10. Phase identification of oxidation products of SU-31 alloy by X-ray diffraction

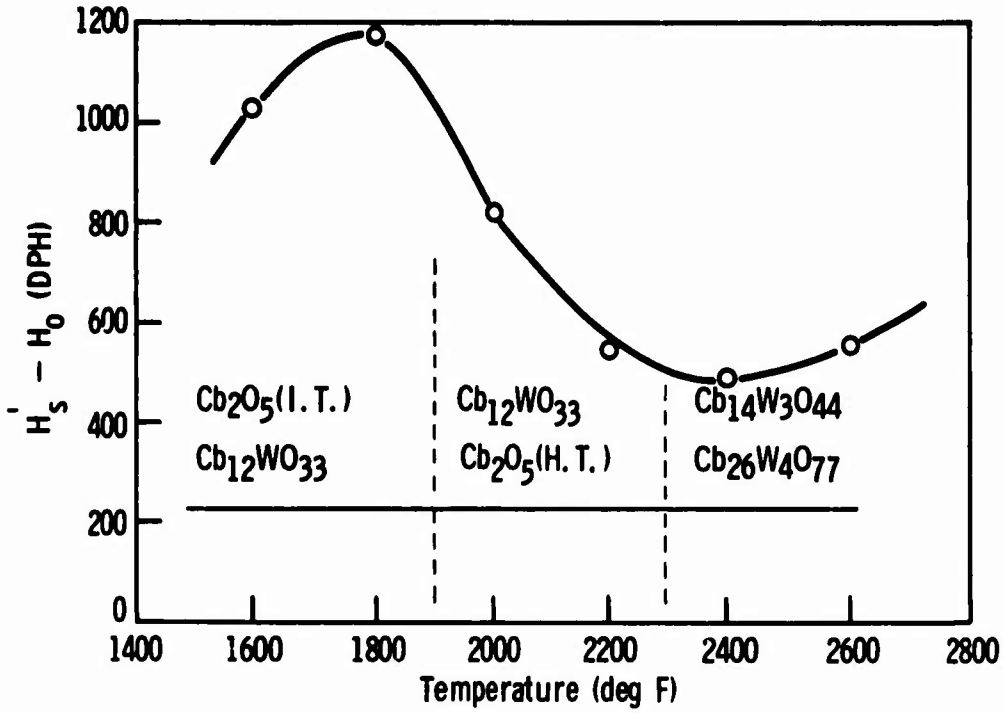

Figure 11. Effect of temperature on surface hardness of oxidized SU-31

eliminated pesting and which was adopted by Solar. Without the post-oxidation treatment, pesting occurs as shown in Figure 12 for FS-85. Note the voluminous reaction products. Pesting appears to be enhanced intercrystalline oxidation of the silicide coating wherein each grain becomes completely surrounded by oxidation products and the material falls apart.

Figure 13 contains oxidation curves for the coated SU-31 alloy between 1600 and 2500 F. No failure occurred in 200 hours at all temperatures studied. Oxidation rates increased with increasing temperature but the total weight gain, even at the highest temperature, is minimal (under 5 mg/cm^2). At 2500 F the dotted portion of the curves shows different behavior. There is a sudden increase in weight probably due to oxidation at a coating defect. However, self-healing of the coating prevents further oxidation, demonstrating that a coating defect need not result in failure even at 2500 F. Similar results were obtained for the FS-85 alloy.

Metallography and Electron Microprobe Analysis

Figure 14 is a photomicrograph of the as-coated SU-31 alloy along with electron microprobe analysis. Point 1 represents the substrate alloy. The coating system is a duplex one having an inner diffusion layer and a porous outermost layer (reservoir layer). Points 2 and 3 are representative of the inner diffusion layer which contains a lower mixed silicide $(Cb, W)_5Si_3$ and a mixed disilicide $(Cb, W)Si_2$. Points 4, 5, and 6 are in the innermost portion of the reservoir layer where the light areas are the mixed disilicides $(Mo, W, Cb)Si_2$ and the darker areas a titanium-rich mixed oxide. The outer portion of the reservoir

19-066-1598/AMC-72

Figure 12. Coated FS-85 after 200 hours of oxidation showing pesting

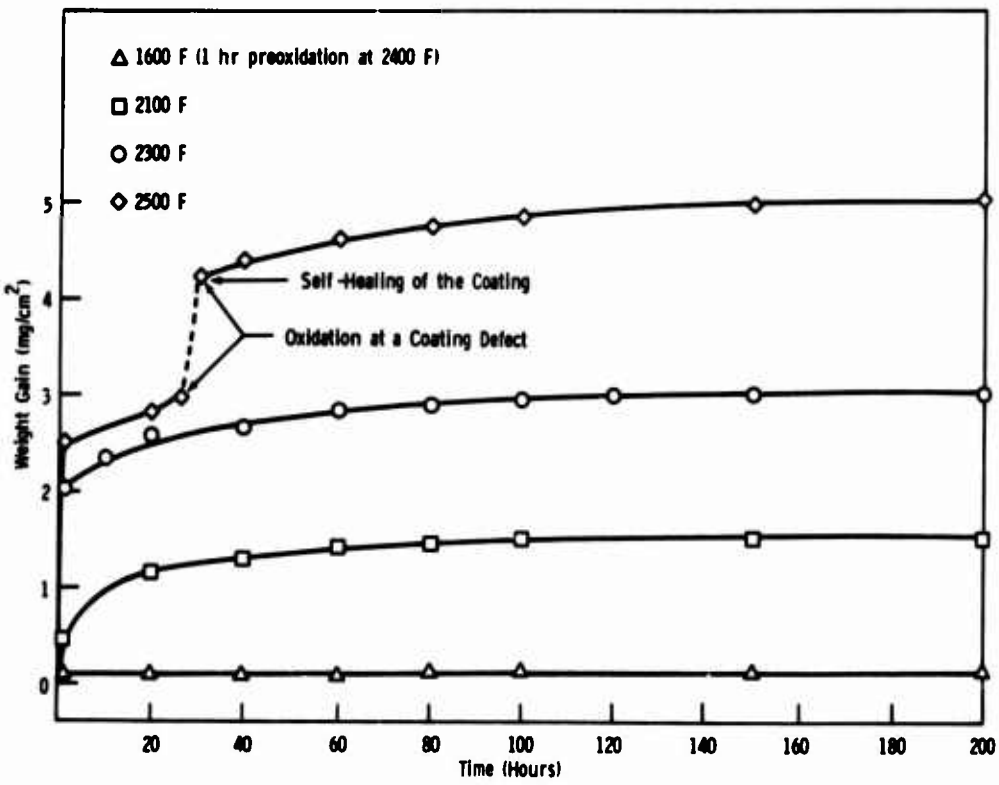

Figure 13. Oxidation of NS4 coated SU-31 between 1600-2500 F

layer is shown at greater magnification to point out that the lightest areas (Point 8) are (W, Mo, V, Ti)Si_2, the darker areas (Point 7) contain (W, Mo)Si_2 and the darkest areas (Point 9) contain SiO_2.

Figure 15 is a photomicrograph of the coated SU-31 alloy which has been oxidized at 1700 F for 200 hours. In addition to the inner diffusion layer and the reservoir layer, a protective outermost layer has been formed which contains both silicon and titanium dioxides. Increasing the temperature of oxidation to 2100 F increases the size of the dense inner diffusion zone as shown in the photomicrograph of Figure 16. The electron microprobe analysis shows that the constituents of the various layers are essentially the same. At 2500 F, within the diffusion layer, more of the lower silicide has formed by conversion of the disilicide, see Figure 17. The lower silicides are not as protective against oxidation as the disilicides. Figure 18, which is also a photomicrograph of the coated SU-31 alloy oxidized at 2500 F for 200 hours, concentrates on the outermost glassy layer of the coating system (dark areas) which is shown filling and sealing a crack that has formed. This glassy layer is increasing in thickness at this temperature and consists mainly of SiO_2 with some Ti in solution and a second dispersed phase of TiO_2.

DISCUSSION

Of the two alloys studied, the SU-31 alloy shows the better oxidation characteristics. However, neither the SU-31 nor the FS-85 alloy has adequate oxidation resistance for gas turbine applications above 2000 F. The oxidation behavior of these alloys is very complex.

Orig. Mag. 500X

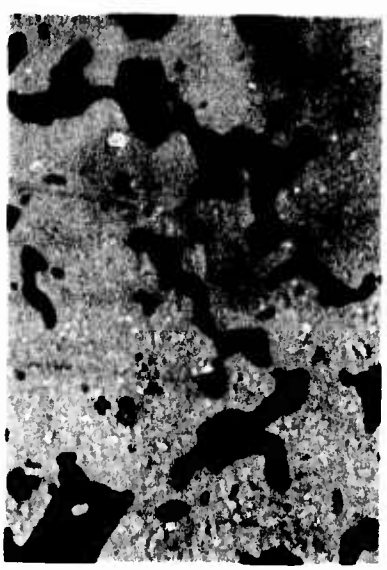

Orig. Mag. 1000X

1. Substrate; 2. (Cb, W)$_5Si_3$; 3. (Cb, W)Si_2;
4. Ti-rich mixed oxide; 5&6. (Mo, W, Cb)Si_2;
7. (W, Mo)Si_2; 8. (W, Mo, V, Ti)Si_2; 9. SiO_2

Figure 14. Microprobe analysis of as-coated system

19-066-1590/AMC-72

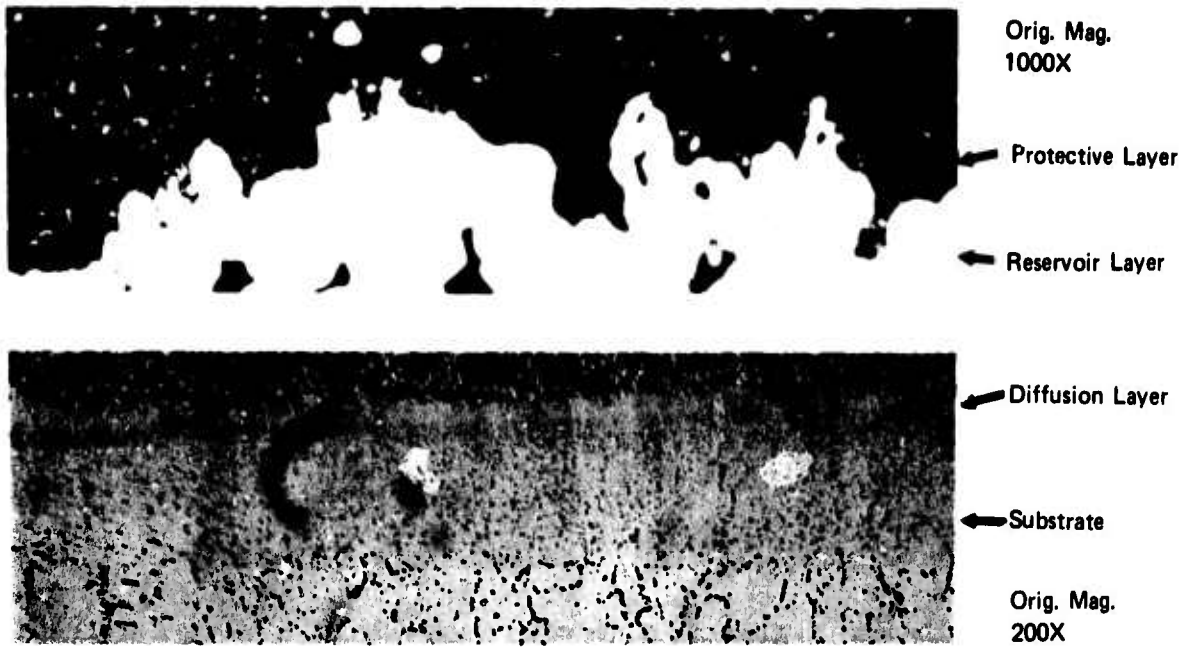

19-066-1597/AMC-72 Figure 15. Coated SU-31 alloy after 200 hours of oxidation at 1700 F

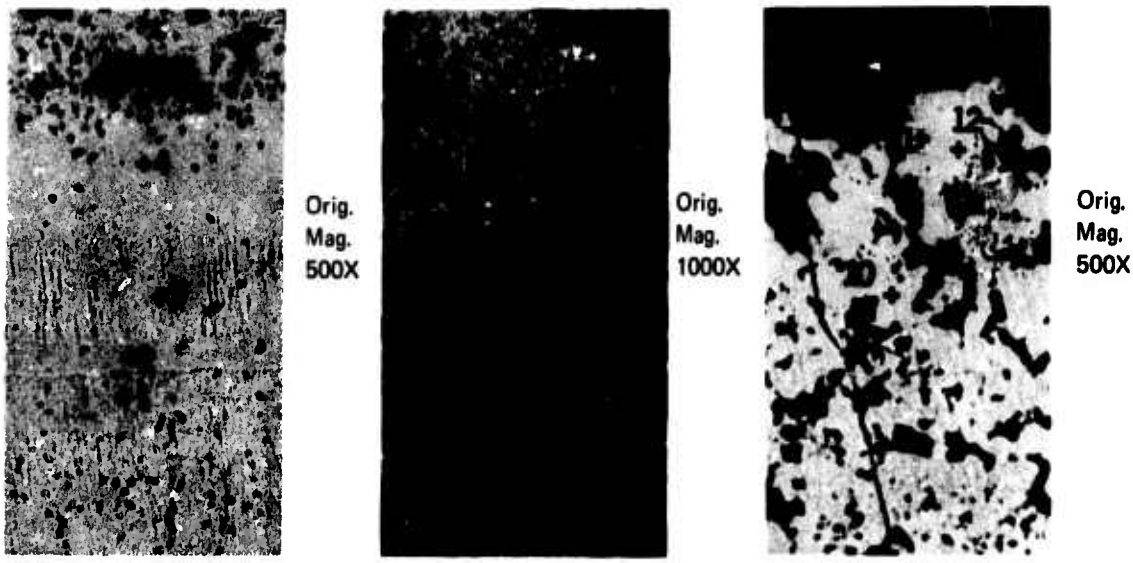

1. Substrate; 2. $(Cb, W)_5Si_3$; 3&4. $(Cb, W)Si_2$; 5. Porous Hf rich oxide; 6,7&8. $(W, Mo, V)Si_2$; 9. Porous SiO_2; 10. $(W, Mo, V, Ti)Si_2$; 11. $(Mo, W, V)Si_2$; 12. $MoSi_2$

19-066-1595/AMC-72 Figure 16. Microprobe analysis after 200 hours of oxidation at 2100 F

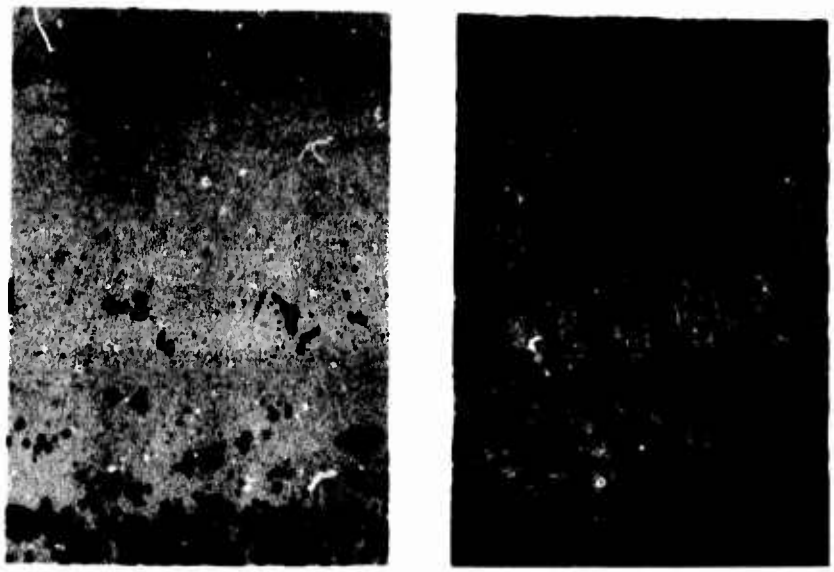

1. Substrate; 2. $(Cb, W)_5Si_3$; 3. $(Cb, W)Si_2$; 4. $(Cb, W, V)_5Si_3$;
5. $(Cb, W, V)Si_2$; 6. $(W, V, Ti, Mo)Si_2$; 7. $(W, Mo)Si_2$; 8. Si-rich oxide

19-066-1594/AMC-72

Figure 17. Microprobe analysis after 200 hours of oxidation at 2500 F. Orig. Mag. 500X

19-066-1591/AMC-72

9. SiO_2; 10&11. Ti-rich oxide; 12&13. Mixed porous oxide

Figure 18. Microprobe analysis after 200 hours of oxidation at 2500 F. Orig. Mag. 200X

Oxidation of SU-31 Alloy

Linear kinetics characterizes the oxidation weight gain curves for SU-31 at 1000 and 1200 F (Figure 3). At these temperatures the formation of CbO_2 was not detected and the oxidation probably proceeds by formation of Cb_2O_5 from CbO_z. However, it appears that the kinetics can be described in terms of mass transport of the oxygen to the surface and the resulting oxide structures and compounds may be only incidental.

At 1400 F the kinetics during the first hour of oxidation of SU-31 change to near parabolic and the formation of CbO_2 was detected. The predominant oxide phases found at both 1200 and 1400 F were the intermediate temperature β Cb_2O_5 and $Cb_{12}WO_{33}$. Thus it appears that for the lower temperature anomaly in SU-31, the change from linear to parabolic kinetics is associated with the formation of the protective CbO_2 suboxide layer, and not with the formation of different modifications of Cb_2O_5 or other final oxide phases.

Increases in temperature between 1400 and 1800 F resulted in accelerated, but still near-parabolic kinetics of oxidation. The high temperature anomaly noted at 2000 F coincides with the change from the intermediate temperature form of Cb_2O_5 to the high temperature form which was observed at 2000 F.

At 2400 and 2600 F, near-parabolic kinetics were observed (Figure 3) at times less than twenty minutes followed by breakaway into a slightly less than linear weight gain with time. The oxide layers at the surface consisted of $Cb_{14}W_3O_{44}$ and $Cb_{26}W_4O_{77}$ which are expected for that temperature range based on the Cb_2O_5-WO_3 binary oxide phase diagram,[18,19] for the alloy composition containing 18.5% tungsten.

Oxidation of FS-85 Alloy

The curves of weight gain versus time for exposure of samples at 1000 to 1300 F are near parabolic in kinetics at the initial stage of oxidation. The tests at 1200, 1300, and 1400 F displayed a marked transition after times of 15 to 20 minutes to a faster than linear region. This behavior corresponds to the transition between stages II and III of the kinetics described by Hurlen[3] for pure columbium.

The presence of a weak diffraction peak associated with CbO_2 was detected in the pattern for the FS-85 specimen exposed at 1600 F. Appearance of the CbO_2 phase coincided with a decrease in slope of the log weight gain versus log time curve from 1.40 for the 1400 F specimens to 0.81 for the 1600 F specimen. While the CbO_2 was first detected on the specimen exposed at 1600 F, it probably did not form a continuous layer. For the specimen exposed at 1700 F, where the CbO_2 diffraction peaks were more pronounced, the slope of the logarithmic plot declined to 0.51. No change in the predominant outer surface oxide phases was noted between 1400 and 1700 F. Therefore, it appears that for FS-85 as well as SU-31, the first or lower temperature anomaly in the temperature dependence of oxidation, which appears in Figures 3 and 4 as a shift from linear to parabolic kinetics, is associated with the formation of CbO_2 as a continuous layer at the metal/oxide interface.

The second or high temperature anomaly in FS-85, which results in the weight gain at 1800 F falling below that for a specimen exposed at 1700 F, coincides with the change in the predominant oxide phase from the intermediate temperature Cb_2O_5 to the high temperature form of Cb_2O_5. While the positions of both the high and low temperature anomalies in FS-85 oxidation weight gain are above the temperatures reported for pure columbium, they correspond well with those reported for binary Cb-Ta alloys[2] of similar tantalum content.

Oxidation of the Coated Alloys

The complex silicide coating afforded both alloys complete protection against static oxidation for at least 200 hours at temperatures up to 2500 F. In fact, no failure occurred at 2500 F for times up to 1000 hours. The excellent oxidation resistance of the coating system is due to the formation of a protective layer which consists mainly of SiO_2 with some Ti, V, and W in solution and a second dispersed phase of TiO_2. While the oxide at and above 2100 F is glassy, the reaction products become increasingly crystalline with decreasing temperature between 1700 and 2000 F.

After the glassy layer is formed, Si and Ti are preferentially oxidized. The oxidation rate curves suggest that the parabolic growth law is applicable indicating that oxide growth is controlled by solid state diffusion through the scale.

During oxidation, the disilicide is partially consumed both by oxidation and by an inward diffusion of silicon. At 2500 F the (Cb, W)Si_2 in the diffusion layer thus becomes converted to (Cb, W)$_5Si_3$. The lower silicide in turn would not exhibit as good oxidation resistance as the disilicides and performance may be reduced.

CONCLUSIONS

1. The SU-31 alloy is more oxidation resistant than the FS-85 alloy. However, neither alloy can be utilized for gas turbine applications above 2000 F without a protective coating.

2. Additional work needs to be carried out in order to test whether mass transport in the gas is rate determining, i.e., calculations of the flux of O_2 molecules striking the alloy surface and a more refined estimate of the sticking probability and the dissociation kinetics.

3. The complex silicide coating completely protects both alloys against static oxidation for at least 200 hours at temperatures between 1600 and 2500 F. In fact, complete protection is afforded the alloys for 1000 hours at 2500 F.

4. Further work is required to evaluate the coating/alloy systems under conditions of cyclic oxidation which more closely simulate gas turbine operation. Also, methods to reduce the thermodynamic activities of diffusing species in the coating should be explored in order to minimize degradation by conversion to lower silicides.

LITERATURE CITED

1. P. Kofstad, "High Temperature Oxidation of Metals", Wiley, New York, 1966, pp. 209-222.

2. I.I. Korobkov, V.V. Osipov, and N.N. Zapleshka, Fiz. Metal. Metalloved, 25 (1968) p. 85.

3. T. Hurlen, J. Inst. Metals, 89 (1960-61) p. 273.

4. E.A. Gulbransen and K.F. Andrew, Trans. Met. Soc. AIME, 188 (1950) p. 586.

5. R.W. Powers and M.V. Doyle, J. Appl. Phys., 30 (1959) p. 514.

6. W.D. Klopp, C.T. Sims, and R.I. Jaffee, Trans. ASM, 51 (1959) p. 282.

7. G. Brauer, H. Muller, and G. Kühner, J. Less Common Metals, 4 (1962) p. 533.

8. R.E. Pawel, J.V. Cathcart, and J.J. Campbell, "Columbium Metallurgy", Metallurgical Society Conf. (AIME), Vol. 10, ed. D.L. Douglass and R.W. Kunz, Interscience, New York, 1961, p. 667.

9. B. Cox and T. Johnston, Trans. Met. Soc. AIME, 227 (1963) p. 36.

10. P. Kofstad and H. Kjollesdal, Trans. Met. Soc. AIME, 221 (1961) p. 285.

11. H. Inouye, "Columbium Metallurgy", Metallurgical Society Conf. (AIME), Vol. 10, ed. D.L. Douglass and R.W. Kunz, Interscience, New York, 1961, p. 649.

12. P. Kofstad and S. Espevik, J. Electrochem Soc., 112 (1965) p. 153.

13. H.J. Goldschmidt, J. Inst. Metals, 87 (1958-59) p. 235.

14. M. Levy and J. Falco, J. Less Common Metals, 27 (1972) p. 43.

15. B.J. Mitchell, Proceeding 6th Annual X-Ray Conf., "Industrial Applications of X-Ray Analysis", 1957, p. 253.

16. R.S. Roth and A.D. Wadsley, Acta Cyrst. 19 (1965) p. 26, p. 32, p. 38.

17. J.J. Falco and M. Levy, J. Less Common Metals, 20 (1970) p. 291.

18. R.S. Roth and J.L. Waring, J. Res. Natl. Bur. Stds., 70A (1966) p. 281.

19. Ceramics Handbook, American Ceramic Society, p. 113.